

## RAMAN SPECTROSCOPY AND RAMAN GAIN COEFFICIENT OF TELLURONIOBIUM- ZINC-LEAD OXYGLASSES DOPED WITH RARE EARTH

EL S. YOUSEF<sup>a\*</sup>, H. H. HEGAZY<sup>a</sup>, M.M. ELOKR<sup>b</sup>, Y. M. ABOUDEIF<sup>b</sup>

<sup>a</sup>*Physics Department, Faculty of Science, Al- Azhar University, Assiut branch, Assiut, Egypt.*

<sup>b</sup>*Physics Department, Faculty of Science, Al-Azhar University, Naser city 11884, Cairo, Egypt.*

The host glasses with composition  $75\text{TeO}_2\text{-}10\text{Nb}_2\text{O}_5\text{-}10\text{ZnO-}5\text{PbO}$  doped with different concentration of  $x\text{Er}_2\text{O}_3$  have been prepared. The structure of the glasses through Raman spectroscopy from 200 to 1300 nm was investigated. The Raman gain coefficients of these glasses evaluated from spontaneous Raman scattering experimental result by using 532 nm Laser type Diode-pumped, solid state (DPSS). The present glasses have broader bandwidths of gain amplification from 225 to  $1125\text{ cm}^{-1}$ . The amplification band width of present glasses is 4.9 times largest than the silica glasses. This indicates that this glass can be use as a potential for fiber Raman amplifier.

(Received September 29, 2015; Accepted December 4, 2015)

*Keywords:* Oxide glasses; Raman spectroscopy; Rare earth

### 1. Introduction

Tellurite glasses used in technological applications such as solid state batteries, fuel cells, gas sensors, infrared filters, optical fibers, modulators and host materials for laser applications [1-3]. Recently in high-speed optical communications, investigation new materials can be increased information flow (short and long distance networks) for an access to new spectral bandwidth are of interest.  $\text{TeO}_2$ - based glasses are a good candidates for these applications; it has broad transmission range from 0.3 to  $5\text{ }\mu\text{m}$  and hence they have highest Raman cross section as compared to other glasses system [4]. Moreover it has Raman gain equal 58 times that of fused silica, which the Raman gain responses evaluate by measuring the Raman spontaneous response [5- 7]. The stimulated Raman scattering is one of the most extensively studied nonlinear optical phenomena applicable to optoelectronic devices such as fiber Raman amplifiers, fiber Raman lasers, microsphere Raman lasers [8], silicon Raman laser [9] and so on. Raman gain media are more advantageous than Rare-earth ions-doped media, since the Raman gain can be obtained at any wavelength depending on the available pump wavelength. In other words, a pump spectrum determines a gain spectrum. Such freedom of the Raman gain spectrum enables advanced devices such as multi-wavelength pumping broadband fiber Raman amplifiers [10] and cascaded Raman lasers [11]. We note that herein the vibration mode of glasses depended on composition and excitation wavelength. Many author [12–22] estimated that the addition of oxides such as  $\text{P}_2\text{O}_5$ ,  $\text{WO}_3$ ,  $\text{Nb}_2\text{O}_5$ ,  $\text{BaO}$ ,  $\text{SrO}$  and  $\text{MoO}_3$  to tellurite glasses leads to expand broad band and high the Raman gain coefficient. In this paper we studied the Raman characteristics of  $\text{TeO}_2/\text{Nb}_2\text{O}_5/\text{ZnO}/\text{PbO}/\text{Er}_2\text{O}_3$  glasses that reveal the highest Raman gain coefficient and broader bandwidth Raman gain amplification compared with other glasses system such as tellurite, silicate, phosphate and borosilicate.

---

\* Corresponding author: [omn\\_yousef2000@yahoo.com](mailto:omn_yousef2000@yahoo.com)

## 2. Experimental

By using the conventional quench-melting method the  $\text{Er}^{3+}$  ions doped glass systems with a composition of  $75\text{TeO}_2\text{-}10\text{Nb}_2\text{O}_5\text{-}5\text{PbO}\text{-}10\text{ZnO}\text{-}x\text{Er}_2\text{O}_3$  (where  $x = 0.00, 2500, 3750, 5000, 6250, 7500$  and  $8750$  ppm) were prepared. The glasses were put in a platinum crucible and melting at  $920^\circ\text{C}$  for 45 min; the crucible was constantly stirred in order to obtain a homogeneous melt. Then the melt was poured onto graphite mould and the quenched samples were annealed at  $320^\circ\text{C}$  for 2 h and then cooled inside the furnace down to room temperature.

The vertical (VV) polarized spontaneous Raman spectra of the prepared glass were acquired using a Thermo Scientific DXR Raman Microscope spectroscopy setup with 532 nm excitation [(532 nm Laser type Diode-pumped, solid state (DPSS))] and acquisition time was set to 30 seconds. The incoming signal vertically surface of the bulk sample, and V-polarized Raman scattered signal was collected in the backscattering geometry with a 100x microscope objective.

## 3. Result and discussion

The prepared glasses excited by using DPSS at wave number ( $\nu_l = 1.880 \times 10^4$  in  $\text{cm}^{-1}$ ) with a power of  $\approx 0.1\text{mW}$ . Herein fig. 1a, b and fig. 2a-h shows the reduced Raman spectroscopy and deconvolution of normalized Raman spectra of prepared glasses respectively. Although the Raman intensity are related to the polarizability of the network modifying ions, the larger polarizable ions contribute more to intensify the high intensity of peak, hence the intensity of Raman spectra increased with increasing of doping  $\text{Er}^{3+}$  ion from 2500 to 8750 ppm. We note that the  $\text{TeO}_2$  network consists of several asymmetric structural units like that  $\text{TeO}_4$  trigonal bipyramids (tbp),  $\text{TeO}_{3+1}$  polyhedra and  $\text{TeO}_3$  trigonal pyramids (tp). Moreover the  $\text{TeO}_4$  group has two axial and two equatorial oxygen atoms, besides the transformation of  $\text{TeO}_4$  tbp convert to  $\text{TeO}_{3+1}$  and  $\text{TeO}_3$  tp units is strongly affected by doping with  $\text{Er}^{3+}$  ions [1, 23]. Also introduction of a network modifier to  $\text{TeO}_2$  based glasses leads to changes the Te coordination polyhedron from  $\text{TeO}_4$  to  $\text{TeO}_3$  through breaking Te-O-Te bonds, along with the formation of non bridging oxygen (NBO) atoms. The Raman bands deconvoluted into six symmetrical Gaussian peaks and the peak position of present glasses were summarized in Table 1. The structure of these glasses investigated as; the band labeled (A) around at  $368\text{-}394\text{ cm}^{-1}$  in sample 2 to 7 can be contributed to the axial bending vibration mode ( $\text{O}_{\text{ax}}\text{-Te-O}_{\text{ax}}$ ) at corner sharing sites, otherwise it is not appeared in sample 1 may be hidden by the strong Raman response of  $\text{TeO}_2$  matrix or of very low intensity. The band as labeled (B) around  $440\text{-}497\text{ cm}^{-1}$  can be attributed to symmetrical or bending vibrations of Te-O-Te linkages at corner sharing sites [28–31]. A band labeled (C) around  $526\text{-}566\text{ cm}^{-1}$  can be attributed to anti symmetrical stretching of the continuous network composed of  $\text{TeO}_4$  tbps [28–31]. A band labeled (D) around  $649\text{-}667\text{ cm}^{-1}$  can be attributed to anti symmetrical stretching of the continuous network composed of  $\text{TeO}_4$  tbps [28–31]. A band labeled (E) around  $755\text{-}807\text{ cm}^{-1}$  can be attributed stretching vibrations of Te-O– and Te=O bonds containing nonbridging oxygen in  $\text{TeO}_3$  tps and  $\text{TeO}_{3+1}$  polyhedra or  $\text{Te}_2\text{O}_7$  bridged tetrahedra (Te-O-Te antisymmetric stretch) [28–33]. A band labeled (F) around  $834\text{-}925\text{ cm}^{-1}$  can be attributed to stretching of Nb and its neighboring NBO in  $\text{NbO}_6$  octahedra [28]. When the concentration of  $\text{Nb}_2\text{O}_5$  content is lower leads to most of  $\text{Te}^{4+}$  ions exist as  $[\text{TeO}_4]$  tbps and form Te–O chains in the glasses matrix, but a few of  $[\text{TeO}_3]$  bps exist in the glass network. The  $\text{Nb}^{5+}$  ions exist as  $[\text{NbO}_6]$  octahedra to link the chains which the apical-sharing  $[\text{TeO}_4]$  tbps are more stable than the edge-sharing ones. Moreover may be  $\text{Nb}^{5+}$  ions in tellurite glasses exist partially in both  $\text{NbO}_6$  octahedra (i.e. connect to non-bridging oxygen, NBO), and  $\text{NbO}_4$  tetrahedra (means that chain to bridging oxygen, BO). Where  $\text{NbO}_4$  tetrahedra take part in as network formers, forming three dimensional structure units contributing to restore bridging bonds and will increase the number of  $\text{TeO}_4$  (tbp) groups just diminishing the  $\text{TeO}_3$  (tp) groups.

Table 1: Glasses composition in mol% and peak position in  $\text{cm}^{-1}$  of prepared glasses.

Sample code	Glasses composition	Peak position in $\text{cm}^{-1}$					
		A	B	C	D	E	F
Sample1	75TeO <sub>2</sub> - 10Nb <sub>2</sub> O <sub>5</sub> - 5PbO- 10ZnO	not appeared	440	not appeared	649	755	869
Sample2	75TeO <sub>2</sub> - 10Nb <sub>2</sub> O <sub>5</sub> - 5PbO- 10ZnO- 2500ppm Er <sub>2</sub> O <sub>3</sub>	368	442	526	679	766	834
Sample3	75TeO <sub>2</sub> - 10Nb <sub>2</sub> O <sub>5</sub> - 5PbO- 10ZnO- 3750ppm Er <sub>2</sub> O <sub>3</sub>	386	493	565	666	803	917
Sample4	75TeO <sub>2</sub> - 10Nb <sub>2</sub> O <sub>5</sub> - 5PbO- 10ZnO- 5000ppm Er <sub>2</sub> O <sub>3</sub>	390	495	566	663	803	919
Sample5	75TeO <sub>2</sub> - 10Nb <sub>2</sub> O <sub>5</sub> - 5PbO- 10ZnO- 6250ppm Er <sub>2</sub> O <sub>3</sub>	394	497	566	664	804	921
Sample6	75TeO <sub>2</sub> - 10Nb <sub>2</sub> O <sub>5</sub> - 5PbO- 10ZnO- 7500ppm Er <sub>2</sub> O <sub>3</sub>	390	496	566	667	807	925
Sample7	75TeO <sub>2</sub> - 10Nb <sub>2</sub> O <sub>5</sub> - 5PbO- 10ZnO- 8750ppm Er <sub>2</sub> O <sub>3</sub>	393	497	566	665	807	925

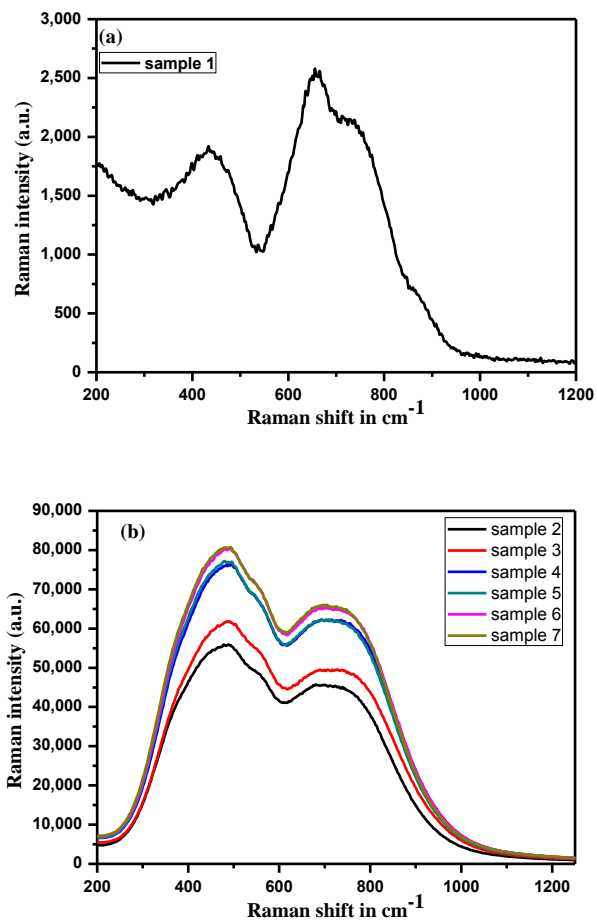


Fig. 1: Raman spectra for studied glasses (a): sample 1 ( $75\text{TeO}_2$ -  $10\text{Nb}_2\text{O}_5$ -  $5\text{PbO}$ -  $10\text{ZnO}$ ), (b) sample 2 ( $75\text{TeO}_2$ -  $10\text{Nb}_2\text{O}_5$ -  $5\text{PbO}$ -  $10\text{ZnO}$  -  $2500\text{ppm Er}_2\text{O}_3$ ), sample 3 ( $75\text{TeO}_2$ -  $10\text{Nb}_2\text{O}_5$ -  $5\text{PbO}$ -  $10\text{ZnO}$  -  $3750\text{ppm Er}_2\text{O}_3$ ), sample 4 ( $75\text{TeO}_2$ -  $10\text{Nb}_2\text{O}_5$ -  $5\text{PbO}$ -  $10\text{ZnO}$ -  $5000\text{ppm Er}_2\text{O}_3$ ), sample 5 ( $75\text{TeO}_2$ -  $10\text{Nb}_2\text{O}_5$ -  $5\text{PbO}$ -  $10\text{ZnO}$ -  $6250\text{ppm Er}_2\text{O}_3$ ), sample 6 ( $75\text{TeO}_2$ -  $10\text{Nb}_2\text{O}_5$ -  $5\text{PbO}$ -  $10\text{ZnO}$ -  $7500\text{ppm Er}_2\text{O}_3$ ), sample 7 ( $75\text{TeO}_2$ -  $10\text{Nb}_2\text{O}_5$ -  $5\text{PbO}$ -  $10\text{ZnO}$ -  $8750\text{ppm Er}_2\text{O}_3$ ).

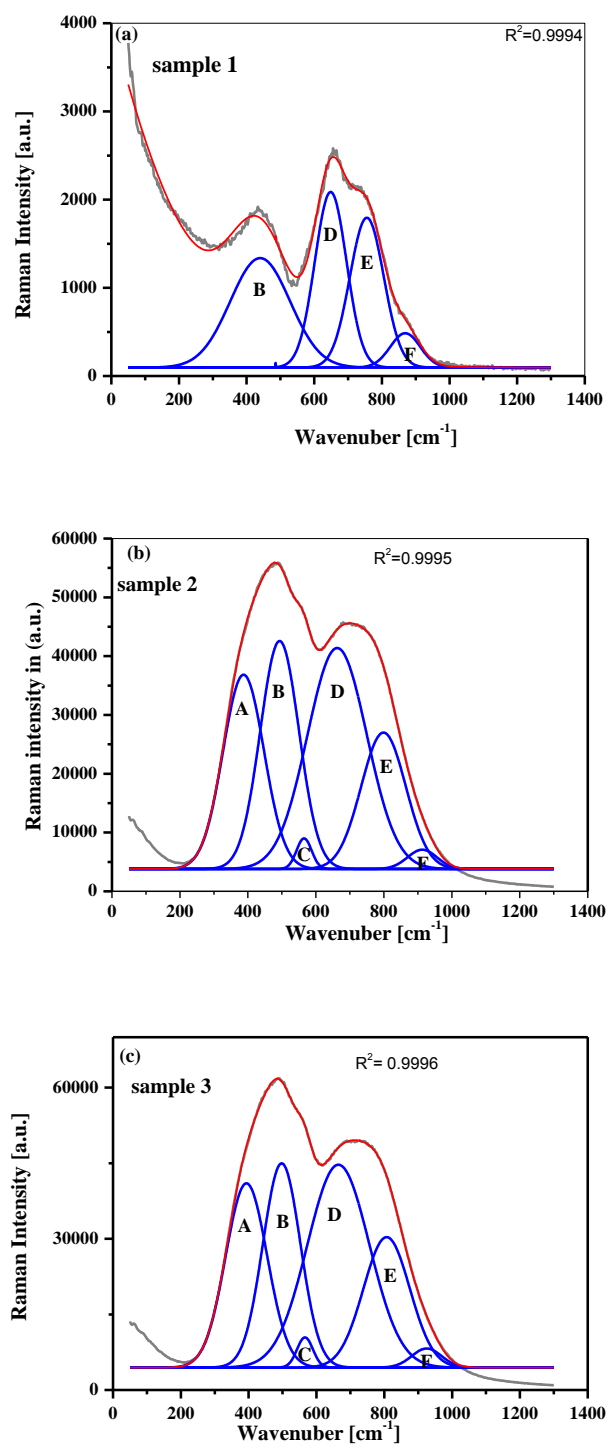


Fig. 2a, b, c: Deconvolution of Raman spectra of prepared glasses (sample 1, sample 2, and sample 3)

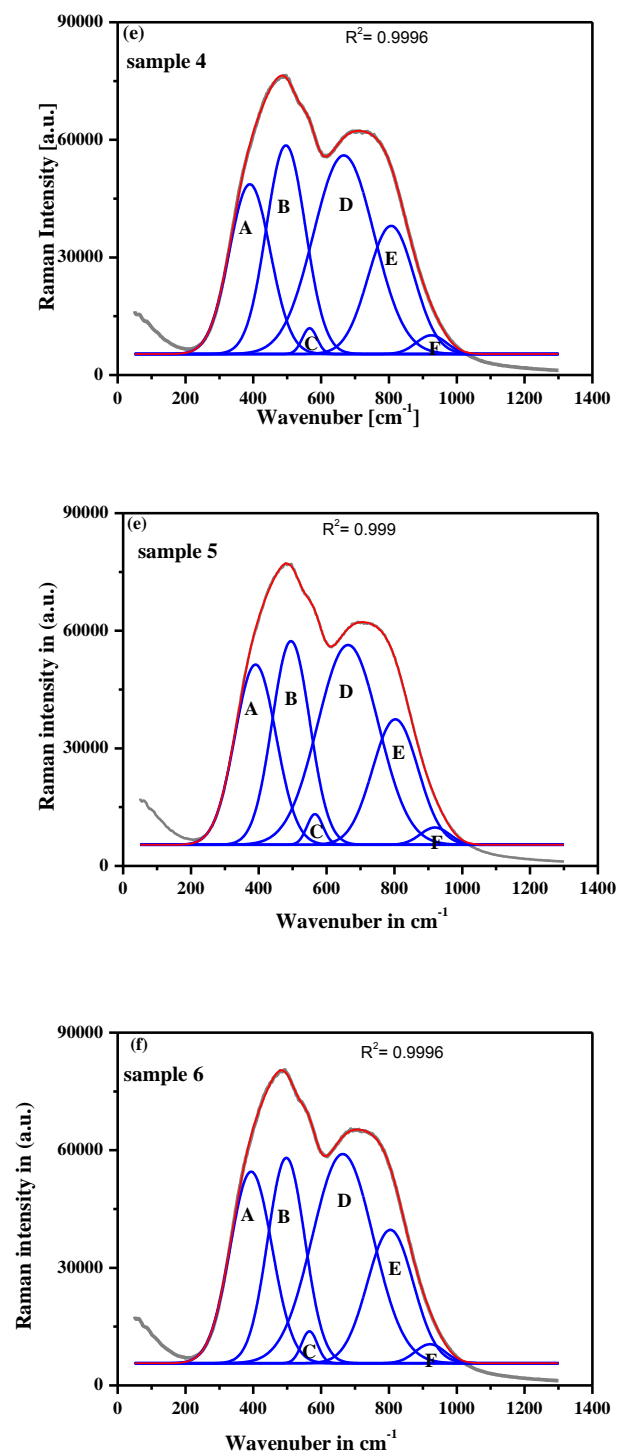


Fig. 2d, e, f: Deconvolution of Raman spectra of prepared glasses (sample 4, sample 5, and sample 6)

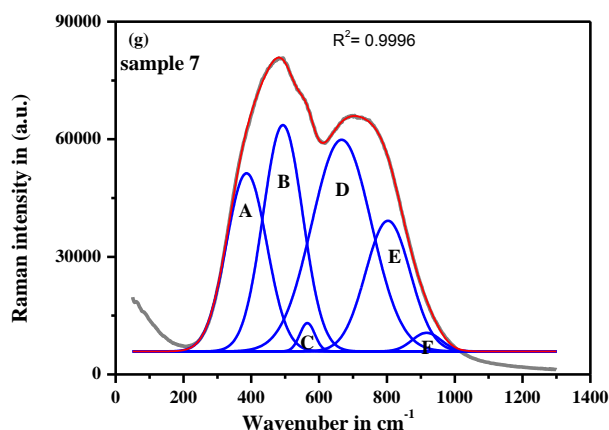


Fig. 2g: Deconvolution of Raman spectra of sample 7.

While the  $\text{Nb}^{5+}$  ions in form of  $\text{NbO}_6$  octahedra occupy interstitial positions as network modifiers. Addition of ZnO content from 0 to 15 wt% in a  $\text{TeO}_2$ - $\text{Nb}_2\text{O}_5$  base glass has two effects on the network structures; (1) it modified few  $\text{Nb}^{5+}$  ions from network modifiers to network formers and increases BO ions, (2) It changes the  $\text{Te}^{4+}$  bond from  $\text{TeO}_4$  tbp to  $\text{TeO}_3$  tp and increases NBO ions. Komatsu and co-workers [34] estimated the bands around 440 and 665  $\text{cm}^{-1}$ , these correspond to Te-O-Te chains and  $\text{TeO}_4$  units in the  $\text{TeO}_2$ - $\text{Na}_2\text{O}$ - $\text{ZnO}$ - $\text{PbO}$  glasses, respectively. Also they reported that when addition of PbO lead to increased the intensity of the band at 765  $\text{cm}^{-1}$  corresponding to  $[\text{TeO}_3]/[\text{TeO}_{3+1}]$  units and PbO at 3 mol%, the lead enters the tellurite network as  $[\text{PbO}_6]$  octahedra. By similarity from the Raman spectra we can calculate the ratio of transform ( $\text{TeO}_4 \rightarrow \text{TeO}_3$  and  $\text{TeO}_{3+1}$ ) in the matrix of studied glasses. The ratio of the value intensity of band (e) to band labeled (d) denotes that fraction ratio  $\text{TeO}_3$  and  $\text{TeO}_{3+1} / \text{TeO}_4$  results were shown in Table (2). From this data the ratio values are in the range from 0.86 to 0.66, this means that the glass without  $\text{Er}_2\text{O}_3$  modifier has highest NBO compared with other glasses doped with rare earth also a result obtain that the  $\text{TeO}_4$  units are transformed little by little to  $\text{TeO}_{3+1}$  and  $\text{TeO}_3$  when increasing  $\text{Er}^{3+}$  ion concentration (see Table 2 column 2). The presence of  $\text{Er}^{3+}$  in these glasses leads to the peak position shift to higher values of wavenumber.

Table 2: Ratio between  $TeO_{3+1}$ ,  $TeO_3$  to  $TeO_4$ , Raman gain coefficients,  $g$ , and full weight half maximum (FWHM) of prepared glasses

Sample code	Ratio of stretching vibrations of Te-O and Te=O bonds containing NBO oxygen in $TeO_3$ tps and $TeO_{3+1}$ polyhedra / BO in $TeO_4$	Raman gain ( $\times 10^{-10} \text{ m.W}^{-1}$ )	FWHM ( $\text{cm}^{-1}$ )
Sample 1	0.86	0.17	252
Sample 2	0.66	3.72	500
Sample 3	0.68	4.2	501
Sample 4	0.68	5.14	496
Sample 5	0.66	5.24	497
Sample 6	0.68	5.43	496
Sample 7	0.66	5.50	500

The reduced spectra in which thermal population and absolute frequency dependence is corrected were obtained using equation:

$$R(w) = \frac{w}{[N(w,T)+1](w_0-w)^4} \cdot I(w) \quad (1)$$

Where  $I(w)$  is the reduced intensity,  $w$  is the Raman shift ( $\text{cm}^{-1}$ ),  $w_0$  is the frequency of the excitation radiation,  $N(w,T)$  is the Bose-Einstein factor,

$$N(w, T) = \frac{1}{\exp\left(\frac{hw}{2\pi K_B T}\right) - 1} \quad (2)$$

Where  $h$  is Planck's constant  $K_B$  is the Boltzman constant, and  $T$  is the measurement temperature (300 K).

The Raman gain spectra can be calculated from spontaneous Raman scattering spectra, the ratio of the number of Stokes photons scattered spontaneously into a solid angle  $d\Omega$  is given by;

$$\frac{d\sigma}{d\Omega} = \left[ \frac{w_s^3 w_p}{(4\pi\epsilon_0 C^2)^2} \right] \cdot \langle |\alpha_R|^2 \rangle \quad (3)$$

Where  $\alpha_R$ = Raman polarizability,  $\epsilon_0$ = permittivity of free space ( $8.8542 \times 10^{-12}$  F/m),  $w_s$ = Stokes frequency,  $w_p$ = pump frequency, C is the speed of light.

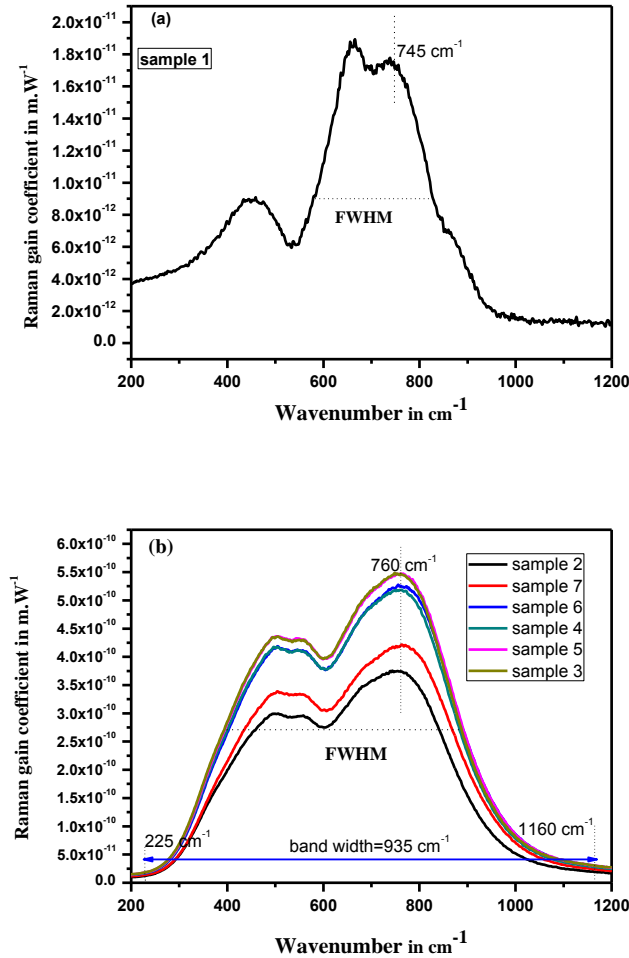


Fig. 3: Raman gain and FWHM for studied glasses (a): sample 1 ( $75\text{TeO}_2$ -  $10\text{Nb}_2\text{O}_5$ -  $5\text{PbO}$ -  $10\text{ZnO}$ ), (b) sample 2 ( $75\text{TeO}_2$ -  $10\text{Nb}_2\text{O}_5$ -  $5\text{PbO}$ -  $10\text{ZnO}$  -  $2500\text{ppm Er}_2\text{O}_3$ ), sample 3 ( $75\text{TeO}_2$ -  $10\text{Nb}_2\text{O}_5$ -  $5\text{PbO}$ -  $10\text{ZnO}$  -  $3750\text{ppm Er}_2\text{O}_3$ ), sample 4 ( $75\text{TeO}_2$ -  $10\text{Nb}_2\text{O}_5$ -  $5\text{PbO}$ -  $10\text{ZnO}$ -  $5000\text{ppm Er}_2\text{O}_3$ ), sample 5 ( $75\text{TeO}_2$ -  $10\text{Nb}_2\text{O}_5$ -  $5\text{PbO}$ -  $10\text{ZnO}$ -  $6250\text{ppm Er}_2\text{O}_3$ ), sample 6 ( $75\text{TeO}_2$ -  $10\text{Nb}_2\text{O}_5$ -  $5\text{PbO}$ -  $10\text{ZnO}$ -  $7500\text{ppm Er}_2\text{O}_3$ ), sample 7 ( $75\text{TeO}_2$ -  $10\text{Nb}_2\text{O}_5$ -  $5\text{PbO}$ -  $10\text{ZnO}$ -  $8750\text{ppm Er}_2\text{O}_3$ ).

The Raman gain coefficient,  $g$ , is related to the spontaneous Raman scattering cross section as [25].

$$g(\nu) = \frac{\sigma(\nu) \cdot \left(\frac{1}{\nu_l - \nu}\right)^3}{c^2 \cdot h \cdot n^2 (\nu_l - \nu)} \quad (4)$$

Where,  $\sigma$ , is the spontaneous Raman cross section. The reported value of the Raman gain coefficient of silica,  $g_{\text{SiO}_2} = 1.86 \times 10^{-13} \text{ m} \cdot \text{W}^{-1}$  at the Stokes shift of  $440 \text{ cm}^{-1}$  for the  $532 \text{ nm}$  excitation [26] was used as the reference. Figure 3a and b, show the Raman gain spectra of prepared glasses. The Raman gain coefficient value at  $760 \text{ cm}^{-1}$  of prepared glasses increase from  $0.17$  to  $5.5 \times 10^{-10} \text{ m} \cdot \text{W}^{-1}$  with increasing  $\text{Er}_2\text{O}_3$  concentration from  $0.0$  to  $8750\text{ppm}$ . The FWHM value of Raman gain increase from  $252$  to  $500 \text{ cm}^{-1}$  with increasing  $\text{Er}_2\text{O}_3$  concentration from  $0.0$  to  $8750\text{ppm}$  (see Table 2). From literature reported in Ref. [28- 33] Raman gain value of the glass  $85\% \text{TeO}_2 - 15\% \text{WO}_3$  and  $85\% \text{TeO}_2 - 10\% \text{Nb}_2\text{O}_5 - 5\% \text{MgO}$  were  $38$  and  $26 \times 10^{-13} \text{ m/W}$  respectively. Raman gain coefficient of  $\text{TeO}_2$ - $\text{ZnO}$ - $\text{Na}_2\text{O}$ ,  $\text{TeO}_2$ - $\text{Na}_2\text{O}$ - $\text{ZnO}$ - $\text{PbO}$ ,  $\text{TeO}_2$ - $\text{WO}_3$ -

$\text{Nb}_2\text{O}_5$  and  $\text{TeO}_2\text{-WO}_3\text{-Bi}_2\text{O}_3$  glasses were found to be 20–30 times that of fused-silica. The broader bandwidth were reported in the tellurite glass containing 15 mol. %  $\text{MoO}_3$  exhibits the bandwidth 1.7 times larger than the silica glass and the Raman gain coefficient is as high as 38 times that of the silica glass. The tellurite glass containing 15 mol %  $\text{MoO}_3$  and 15 mol %  $\text{P}_2\text{O}_5$  shows the bandwidth 1.9 times larger than the silica glass and high Raman gain coefficient which is as high as 37 times that of the silica glass. In the present work the prepared glasses has highest value of Raman gain coefficient compared with other glasses were reported in the literature [28-33]. Moreover these glasses have bandwidth as high as 4.9 times larger than the silica glass. Hence this indicates that this glass can be used in gain media such as broadband Raman amplifier. The formation  $\text{TeO}_3$  and  $\text{TeO}_{3+1}$  units at  $760\text{ cm}^{-1}$ ,  $\text{Nb}^{5+}$ ,  $\text{Pb}^{2+}$  and  $\text{Er}^{3+}$  may be are character more polarizability ion in this glasses matrix than compare with other glasses leads to higher Raman gain.

#### 4. Conclusion

High polarizability oxide  $\text{PbO}$  and  $\text{Er}^{3+}$  ion added to host glass matrix with composition  $\text{TeO}_2\text{-Nb}_2\text{O}_5\text{-PbO-ZnO}$  leads to getting high Raman spectra intensity, Raman gain coefficient and extend the bandwidth amplification. Characteristic units for  $\text{TeO}_4$ ,  $\text{TeO}_{3+1}$  and  $\text{TeO}_3$  phases were detected in the structure of the investigated glasses. The fraction ratio between  $\text{TeO}_3$  and  $\text{TeO}_{3+1}$  phase to  $\text{TeO}_4$  decreases from 0.86 to 0.66 with doping  $\text{Er}^{3+}$  ion.  $75\text{TeO}_2\text{-}10\text{Nb}_2\text{O}_5\text{-}5\text{PbO-}10\text{ZnO-}8750\text{ppm Er}_2\text{O}_3$  has the highest value of Raman gain coefficient equal  $5.5 \times 10^{-10}\text{ m}\cdot\text{W}^{-1}$  and bandwidth as high as 4.9 times larger than the silica glass.

#### Acknowledgements

This work was financially supported by the Department of Physics, Faculty of Science, Al- Azhar Univ., Cairo Branch, Egypt.

#### References

- [1] C. Duverger, M. Bouzaoui, S. Turrell, J. Non-Cryst. Solids **220**,169 (1997).
- [2] K. Muruganandam, M. Seshasayee, J. Non-Cryst. Solids **222**,131 (1997).
- [3] P. Charton, P. Armand, J. Non-Cryst. Solids **333**,307 (2004).
- [4] K. Damak, E. Yousef, S. AlFaify, C. Rüssel, R. Maâlej, OPTICAL MATERIALS EXPRESS **4**(4), 598 (2014).
- [5] Kamel Damak, El Sayed Yousef, Christian Rüssel, Ramzi. Maâlej, Journal of Quantitative Spectroscopy & Radiative Transfer **134**,55 (2014).
- [6] El Sayed Yousef, Journal of Alloys and Compounds **561**,234 (2013).
- [7] C. Rivero, R. Stegeman, M. Couzi, D. Talaga, T. Cardinal, K. Richardson, G. Stegeman, Opt. Express **13**(12),4759 (2005).
- [8] S. Spillane, T. Kippenberg, K. Vahala, Nature **145**,621 (2002).
- [9] M El-Okr, M Ibrahim, M Farouk, J. Phys. Chem. Solids **69**,2564 (2008).
- [10] M El Okr, M Farouk, M El-Sherbiny, MAK El-Fayoumi, MG Brik, J. Alloys Comp. **490**(1), 184 (2010).
- [11] E.M. Dianov, I.A. Bufetov, M.M. Bubnov, M.V. Grekov, S.A. Vasiliev, O.I. Medvedkov, Opt. Lett. **25**,402 (2000).
- [12] L.F. Mollenauer, R.H. Stolen, M.N. Islam, Opt. Lett. **10**,229 (1985).
- [13] A. Mori, H. Masuda, K. Shikano, K. Oikawa, K. Kato, M. Shimizu, Electron. Lett **37**,1442 (2001).
- [14] A. Mori, H. Masuda, K. Shikano, K. Oikawa, K. Kato, M. Shimizu, J. Lightwave Technol. **21**,1300 (2003).
- [15] R. Jose, Y. Ohishi, Appl. Phys. Lett. **90**,211104-1 (2007).

- [16] D.R. Ulrich, *J. Am. Ceram. Soc.* **47**, 595 (1964).
- [17] J.S. Wang, E.M. Vogel, E. Snitzer, *Opt. Mater.* **3**, 187 (1994).
- [18] G.S. Murugan, T. Suzuki, Y. Ohishi, *Appl. Phys. Lett.* **86**, 161109-1 (2005).
- [19] G.S. Murugan, T. Suzuki, Y. Ohishi, *Frontiers in Optics, OSA Technical Digest Series*, Optical Society of America, 2004, p. FMB4.
- [20] R. Jose, T. Suzuki, Y. Ohishi, *J. Non-Cryst. Solids* **352**, 5564 (2006).
- [21] R. Jose, Y. Arai, Y. Ohishi, *J. Opt. Soc. Am. B* **24**, 1517 (2007).
- [22] R. Jose, G. Qin, Y. Arai, Y. Ohishi, *J. Opt. Soc. Am. B* **35**, 373 (2008).
- [23] R. F. Cuevas, L. C. Barbosa, A. M. de Paula, Y. Liu, V. C. S. Reynoso, O. L. Alves, N. Aranha, C. L. Cesar, *J. Non-Cryst. Solids* **191**, 107 (1995).
- [24] A.E. Miller, K. Nassau, K.B. Lyons, M.E. Lines, *J. Non-Cryst. Solids* **99**, 289 (1988).
- [25] R.H. Stolen, E.P. Ippen, *Appl. Phys. Lett.* **22**, 276 (1973).
- [26] R.H. Stolen, C. Lee, R.K. Jai, *J. Opt. Soc. Am. B* **1**, 652 (1984).
- [27] F.L. Galeener, P.N. Sen, *Phys. Rev. B* **17**(4), 1928 (1978).
- [28] G.S. Murugan, Y. Ohishi, *J. Appl. Phys.* **96**, 2437 (2004).
- [29] T. Sekiya, N. Mochida, A. Ohtsuka, *J. Non-Cryst. Solids* **168**, 106 (1994).
- [30] T. Sekiya, N. Mochida, A. Ohtsuka, A. Soejima, *J. Non-Cryst. Solids* **151**, 222 (1992).
- [31] T. Sekiya, N. Mochida, A. Soejima, *J. Non-Cryst. Solids* **191**, 115 (1995).
- [32] T. Uchino, T. Yoko, *J. Non-Cryst. Solids* **204**, 243 (1996).
- [33] S. Suehara, S. Hishita, S. Inoue, A. Nukui, *Phys. Rev.* **56B**, 14124 (1998).
- [34] T. Komatsu, H. G. Kuin, and H. Mohri, *J. Mater., Sci. Lett.* **15**, 2026 (1991).